International Journal of Mechanical, Industrial and Aerospace Sciences
ISSN: 2517-9950
Vol:11, No:4, 2017

Study on Bending Characteristics of Square Tube Using Energy Absorption Part

Shigeyuki Haruyama, Zefry Darmawan, Ken Kaminishi

Abstract**—**In the square tube subjected to the bending load, the rigidity of the entire square tube is reduced when a collapse occurs due to local stress concentration. Therefore, in this research, the influence of bending load on the square tube with attached energy absorbing part was examined and reported. The analysis was conducted by using Finite Element Method (FEM) to produced bending deflection and buckling points. Energy absorption was compared from rigidity of attached part and square tube body. Buckling point was influenced by the rigidity of attached part and the thickness rate of square tube.

Keywords**—**Square tube, bending stress, energy absorption, finite element analysis, rigidity.

I. Introduction

A system with supported by reinforcing structures was widely used everywhere. Many construction buildings, machinery, and engineering system deploy structures support as the structure. Structure has many shapes; square, tubular, polygonal, and others. Engineers have to increase the ability of structure over the strength through its mechanical properties. Experiments were conducted many ways to produce high strength material as supported structure. The solid material has most strength compared with hollow, however, the solid consumes more material and leads to high production cost [1]-[3]. High strength with low weight was a superior combination as various structures. Tube shape was preferred to reduce weight and pretends as solid strength [4].

Square tubes have many theoretical and experimental studies. Kecman [5] studied about bending collapse behavior subjected to bending load of square tubes. A theoretical analysis was compared with experimental result and found that plastic deformation was obtained between two stable segments. Johnson [6] also showed a mathematical solution of the bending and torsion of an anisotropic elastic beam. It is shown that bending stiffness is greater when twisting is banned. Kim et al. [7] suggested a new approach of collapse mechanism that improved the relationship between moment-rotation. The new solution determines two unknown constants, half-length of folding wave and rolling radius by reducing a mean crumpling moment. Further study about bending was specifically focused on flattening deformation in rectangular hollow structure [8]. The relationship between flattening ratio and non-dimensional curvatures was influenced by tube thickness [9].

Haruyama et al. [10] explored about axially tubular crush so-called compress-expand part to investigate energy absorption using FEM and experiments. Thin wall cylindrical tube crushed impact was used and modeled as absorption energy at impact test. Collapse mode can be divided into three groups, stable mode, stable with a folding mode, and unstable mode. Moreover, [11] studied about compress-expand part under axial loading using finite element analysis and plotted various modes of member's collapse according to the geometric and material parameter. It seems that compress-expand member had most efficiency in the smaller radius.

In this paper, the study was focused on bending behavior of square tubes using attached part to absorb bending stress at lateral side and transmit to attach part at axial side of stress. Energy absorption of attached part investigated to influence buckling point of square tube and rigidity force of absorption part.

II. Methodology

This research developed a basic model of the square tube for bending loading analysis. A compress-expand part was attached at end side of tube as energy absorber when deflection occurs during bending. Fig. 1 shows the square tube model. For analysis purposes, a model of absorption part was created. Characteristic of absorption part was equal to tubular crush with three pieces section. Fig. 2 shows analogical model of square tube with attached part as spring. Materials of square tube and absorption part were homogeneous and isotropic elastic-plastic which followed rule (1):

$$\begin{aligned} \sigma &= E\varepsilon \quad \left[\varepsilon < \frac{\sigma_y}{E}\right] \\ \sigma &= \sigma_y + E_h\left(\varepsilon - \frac{\sigma_y}{E}\right) \quad \left[\varepsilon > \frac{\sigma_y}{E}\right] \end{aligned} \tag{1}$$

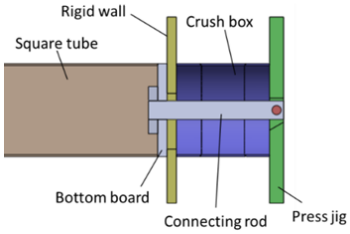

Fig. 1 Square tube model

Parameters and material properties of square tube are shown in Table I. Material properties of absorption part followed Fig.

Shigeyuki Haruyama and Ken Kaminishi are with graduate School of Innovation and Technology Management, Yamaguchi University, Ube, Japan (e-mail: haruyama@yamaguchi-u.ac.jp, kaminisi@yamaguchi-u.ac.jp).

Zefry Darmawan is doctoral student at Department of Mechanical Engineering, Yamaguchi University, Japan and staff at Industrial Engineering, University of Brawijaya-Indonesia (e-mail: v501wc@yamaguchi-u.ac.jp).

3. It was identical to tubular crush box with three pieces (2 compress and 1 expand member). Parameters of absorption part are shown in Table II.

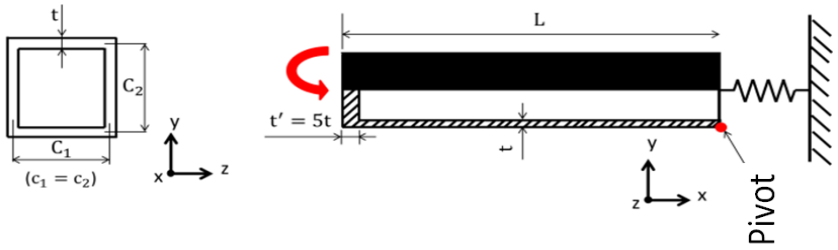

Fig. 2 Analogical model

TABLE I
PARAMETER OF SQUARE TUBE

Parameter	Value
Length L (mm)	1000
Width C1(=C2) (mm)	100
Thickness t (mm)	1,2,3,4,5,6
Modulus E (GPa)	205.9
Poisson v	0.3
Work hardening Eh/E	1/100
Yield stress σ (E/1000) (MPa)	205.9

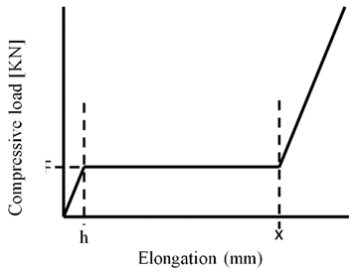

Fig. 3 Absorption part characteristic

TABLE II
PARAMETER OF ABSORPTION PART

Parameter	Value
Constant (a)	0.2, 0.4, 0.6, 0.8
Elongation (x) [mm]	10, 20, 30
Shape factor (t/C1)	0,01; 0,02; 0,03; 0,04; 0,05; 0,06

Absorption model was characterized as seen at (2):

$$F = a\, P_{cr}\ [KN]$$
$$P_{cr} = \sigma_{cr} \,.\, A \qquad (2)$$

where, F is rigidity force of attached part, P_{cr} is collapse rate force at cylindrical compress-expand member tube, and A is the rectangular cross section area of the tube.

III. RESULT

Software MSC Marc was used to perform finite element simulation, the result of moment M [N.m] and bending stress α_x[MPa] on the square tube as seen in Fig. 5. The horizontal axis represents non-dimensional curvature and vertical axis shows bending stress. A square tube without absorption part was analysed as the basic comparison for tube equipped with absorption part.

There are several collapse mode of the square tube; side collapse, bottom collapse, and flat type. Each collapse figure was obtained from section A-A of square tube, as shown in Fig. 4.

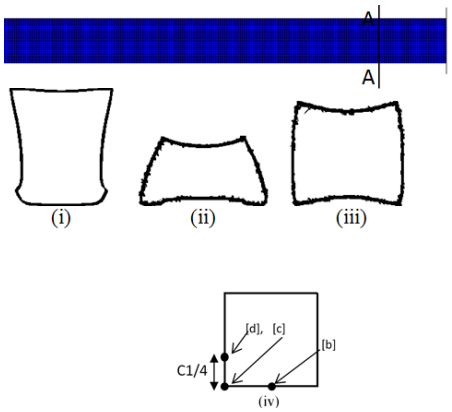

Fig. 4 Collapse mode; (i). side collapse; (ii). bottom collapse; (iii). Flat collapse mode; (iv). observation area; Observation area of cross-section square tube divide into; [b] center point, [c] corner point, [d] edge point

The simulation result showed buckling at side collapse and bottom collapse, but flat collapse not occurred buckling. Fig. 5 shows the transition of axial compressive stress α_x[MPa] between the center point (B) and corner point (C) on the compression side of the bending moment and the surface where wrinkles are generated. The bending moment M[N.m] and the axial stress α_x[MPa] of the point B are maximum at ①. When the bending moment M starts to decrease in ②, immediately the deformation of the center section (B) progresses and the stress at the point B decreases. From this, it is considered that the maximum bending moment appeared due to buckling of the compression side surface.

Fig. 6 shows relationship between bending moment M[N.m] and curvature κ[m^{-1}] at flat collapse mode. The transition of the compressive stress α_x[MPa] in the axial direction at the center point (B) and the corner point (C) on the compression side were the critical points. The bending moment M continues to increase even when point (B) reaches the maximum stress in ①. Then, stress at the point (B)

decreases, but the stress at the corner point (C) rises. From this, it is considered that the bending moment increased even after the stress at the point (B) decreased since the rate of stress rise was greater than the rate of stress reduction at the compression side.

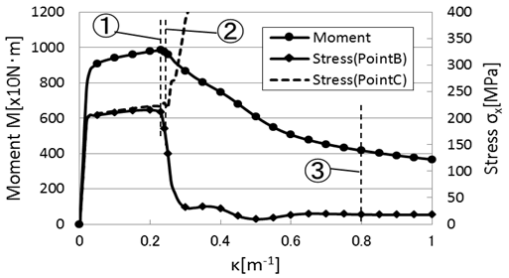

Fig. 5 Moment-Stress comparison at buckling collapse mode (E_h/E=0.01; t/C_1=0.03)

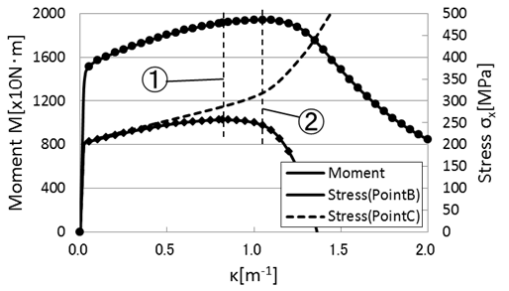

Fig. 6 Moment-Stress comparison at flat collapse mode (E_h/E=0.01; t/C_1=0.05)

Each absorption part with rigidity force produced different maximum bending stress compared with square tube without absorption part. Comparisons of bending stress are shown at Table III.

Maximum bending stress was obtained at square tube without absorption part and the smallest bending stress obtained from a square tube with absorption part $0.2P_{buc}$.

The result of bending on square tube also classified based on collapse mode. Effects of the rigidity force are obtained as follows.

A. Side Collapse Mechanism

Fig. 7 shows the transition of the axial compressive stress α_x[MPa] and the spring work W[N.mm] of the center point (B) and the edge point (D). Compressive stress was taken as positive. A deformed line (1-4) was created to show specific deformation of square tube. The stress value at the center point (B) of the compression side reaches its maximum at ① and turns into decrease, but the spring work continues to increase. This indicates that the cause of collapse is not due to deformation of the point (B). Thereafter, when the spring work reaches the maximum in ②, the axial stress at the point (D) becomes the maximum, and when the spring work decreases at ③ the stress at the point (D) also decreases. From this, it is considered that the spring work maximized the buckling point at the edge surface.

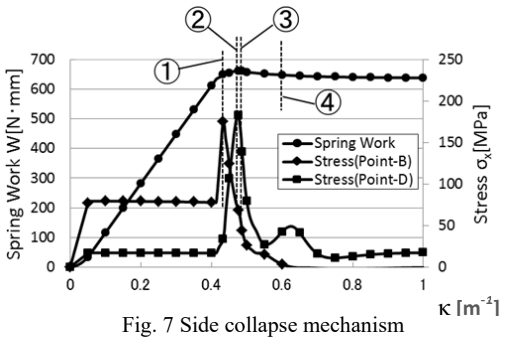

Fig. 7 Side collapse mechanism

TABLE III
BENDING STRESS COMPARISON

Rigidity force F=[KN]	Max Bending stress [MPa]	Curvature [m^{-1}]
Square tube only	215.5	0.19
0.2 P_{buc}	202.2	0.61
0.4 P_{buc}	207.2	0.54
0.6 P_{buc}	207.2	0.52
0.8 P_{buc}	206.5	0.14

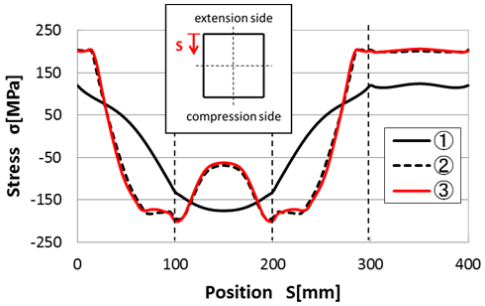

Fig. 8 Cross-sectional stress of side collapse

Fig. 8 shows a cross-sectional stress σ[MPa] diagram at ①-③. The stress σ at the center side (B) decreases after reaching the maximum, but the stress σ on the side surface (D) rises from the corner on the compression side, so that the stress on the center side exceeds the decrease amount and the spring work increases. It seems that the resultant force on the side surface becomes the maximum at ②; the spring work becomes the maximum.

B. Bottom Collapse Mechanism

Fig. 9 shows the transition of axial compressive stress σ_x[MPa] between the center point (B) and corner point (C) on the compression side of the surface where spring work and wrinkles are generated. The spring work W[N.mm] and the axial stress α_x[MPa] of the point (B) are reach maximum at ①. When the spring (W) starts to decrease at ②, immediately the stress σ_x at the point B decreases. From this, it is considered that the spring work W increased buckling point of the center side surface.

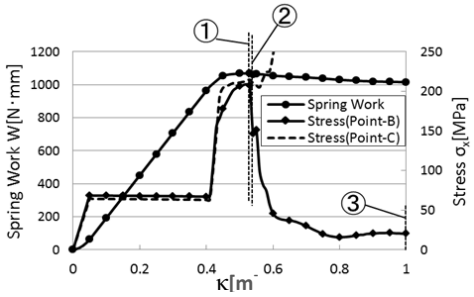

Fig. 9 Bottom collapse mechanism

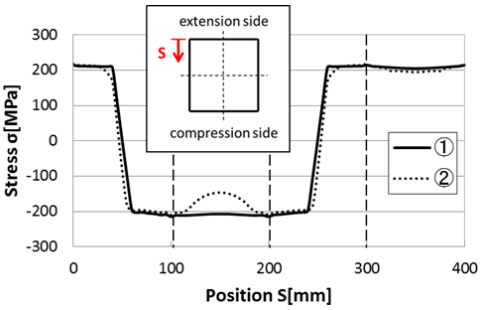

Fig. 10 Cross-sectional stress of bottom collapse

In order to confirm that the stress σ at point B decreased, Fig. 10 shows the stress distribution diagram at the buckling surface in ①, ②. It is found that the absolute values of the stresses of the extension surface and the compression surface are equal and uniformly distributed. Thereafter, in ②, the stress distribution of the extension surface hardly changes, but the absolute value of the stress of the compression surface decreases, which indicates that buckling occurs. And as deformation progresses, wrinkles are generated as shown in the deformation chart in ③.

C. Flat Collapse Mechanism

Fig. 11 shows the relationship between spring work W[N.mm] and curvature κ[m^{-1}] and the transition of axial compressive stress. The spring work continues to increase even after point (B) has reached the maximum stress in ①. While spring work W starts to decrease at ②, stress at point (C) continue to increase.

As shown in Fig. 12, when ① and ② are compared, the stress σ at the compression side decreases but the stress at the corner point (C) rises. From this, it is considered that the spring work increased even after the stress at the point (B) decreased, since the rate of stress increase was larger than the rate of stress reduction on the compression side. Also, it can be seen that the deformation of the extension side and the compression side is the same. The stress distributions of the extension side (S = 300 to 400 [mm]) and the compression side (S = 200 to 300 [mm]) are substantially the same. From this, it is clearly that no buckling occurs.

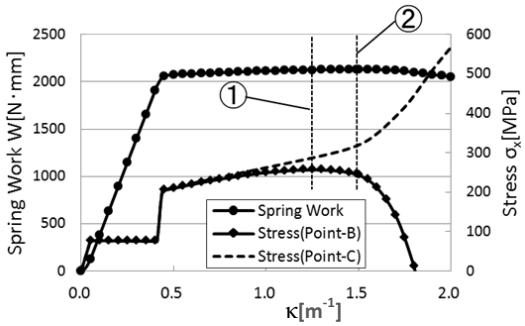

Fig. 11 Flat collapse mechanisms

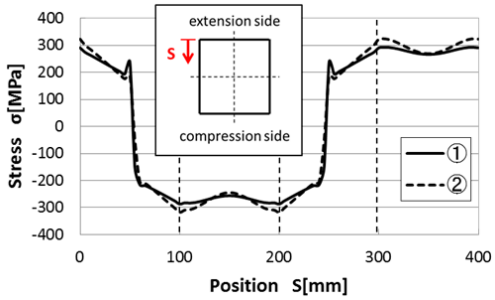

Fig. 12 Cross-sectional of flat collapse

Since the spring element is used instead of the energy absorbing member, it is impossible to evaluate the energy after collapse where the elongation of the spring decreases. Therefore, we investigate the amount of energy absorption up to the collapse. The energy absorption E is evaluated by the sum of the strain energy (U) of the rectangular tube and the spring energy (W) performed by the absorption element. (3) and (4) are equations of the energy absorption where V is the volume [Liter], P is the force of the spring [N], and δ is the elongation of the spring [mm].

$$U = V \int \sigma_{ij} \varepsilon_{ij} \tag{3}$$

$$W = \int P d\delta \tag{4}$$

We compare the energy absorption amount of each deformation mode in the square tube where the spring element is applied. Fig. 13 shows the relationship between the energy increment ΔE/κ and the curvature κ[m^{-1}] until each deformation mode leads to collapse.

From Fig. 13, the increasing trend is the same in all deformation modes up to ②. Specifically, in ① the spring extends to h, ① ~ ② while h is increase, the spring force is constant. After that, the elongation of the spring becomes x in ② (elongation of h and x follow Fig. 3). After ② the deformation of the rectangular tube starts, leading to the collapse. As compared with the energy absorption amount, it is clear that the flat type has a larger amount of energy than the bottom type. Because wall thickness of the flat-type mode is thicker than the bottom-type mode, the rigidity is high. For the latter, the equivalent plastic strain distribution is shown in

Fig. 14 for comparison.

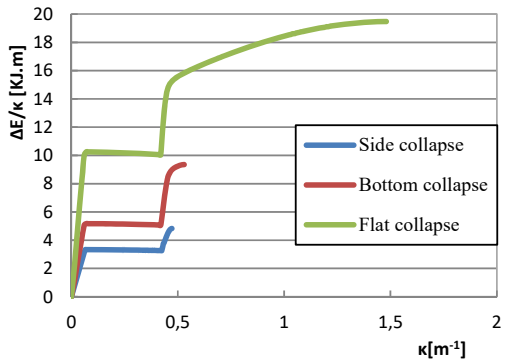

Fig. 13 Energy base on collapse mode

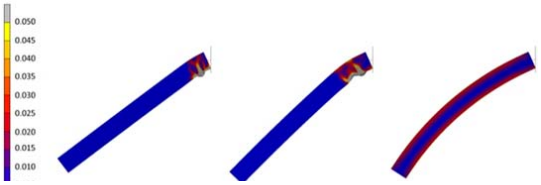

Fig. 14 Equivalent plastic strain distributions

From Fig. 15, it can be seen that the buckling type locally concentrates the strain, whereas the flat type has the distortion occurring in the wide range. Influence on the amount of energy absorption due to the presence or absence of a spring obtained at Fig. 15.

Fig. 15 shows the relationship between the increment of energy ΔE/κ[kJ.m] and the curvature κ[m^{-1}]in a rectangular. From this, it can be seen that applying the spring increases the amount of deformation required until the collapse, but the maximum value of the energy increase is decreasing. In order to confirm this fact, the changes of the total energy absorption amount and the spring work increment ΔE/κ, ΔW/κ in the bottom type and the flat type are shown in Figs. 16 and 17.

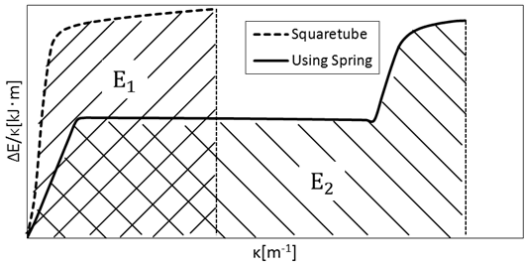

Fig. 15 Influence of spring at square tube bending

In the flat type, the strain energy increases due to deformation of the spring. Then spring deformation continues decrease then deformation at tube start occurs. Result of the total energy absorption increase until collapse.

Deformation at side collapse mode shows contrast result than flat collapse mode. According to Figs. 16 and 17, relation between the spring work W and the strain energy U at flat collapse is W<U. The bottom collapse is W>U. Therefore, it can be said that the bottom type has a potential area of absorption energy applying the spring.

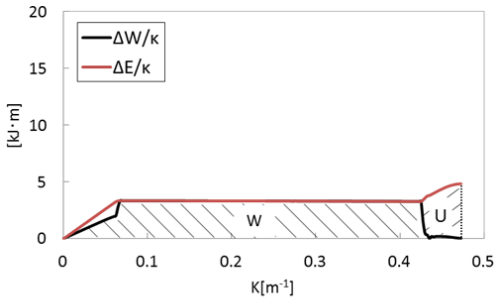

Side collapse

Fig. 16 Absorption energy at side collapse mode

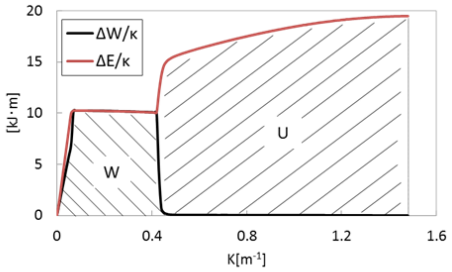

Flat collapse

Fig. 17 Absorption energy at flat collapse mode

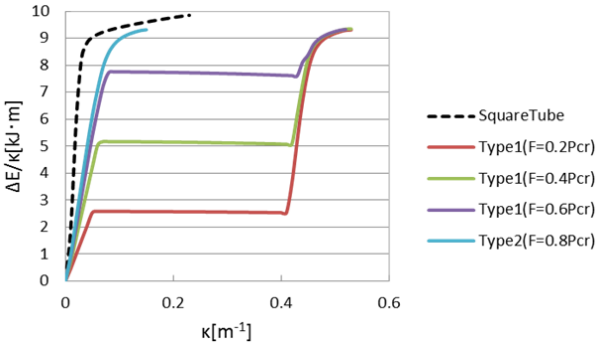

Fig. 18 Energy comparisons at various F rate

Can be seen from Fig. 18, in Type 1, as the elongation of the spring reaches h, the increasing amount of the spring work becomes constant, and when the elongation becomes x, the deformation of the rectangular tube starts and the spring work decreases. In Type 2, the deformation of the rectangular tube begins before the elongation of the spring becomes h, so the increment of the spring work is not constant but decreases. From this, it can be said that the spring is not functioning sufficiently for Type 2.

From Fig. 19, it shows that only type 1 which the spring work is performed within the range where the increment of the

energy is constant, so that the magnitude of the increase amount in this range depends on F. Further, it is confirmed that spring work at type 2 not provide significant result to increase energy amount.

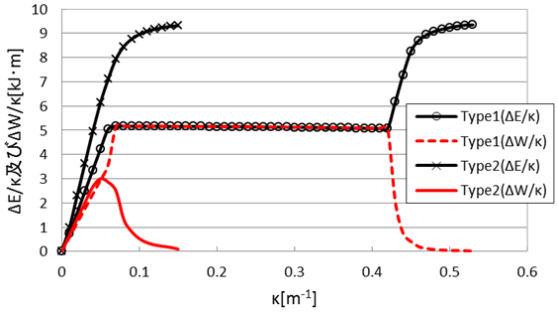

Fig. 19 Different energy characteristics in type 1 and 2

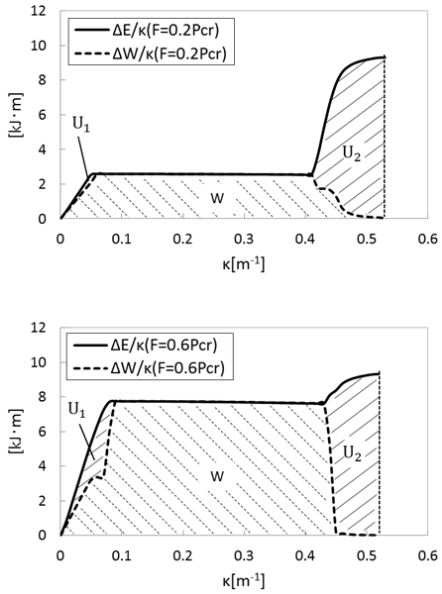

Fig. 20 Comparison energy between F=0,2P_{cr} and F=0,6P_{cr}

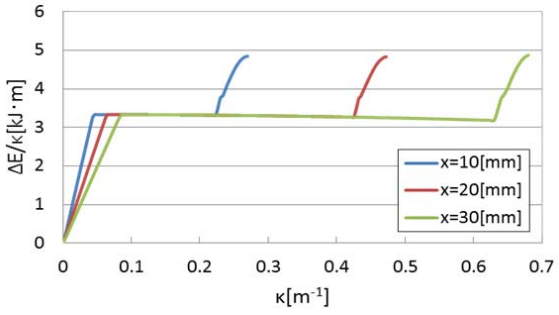

Fig. 21 Energy characteristic due to change x amount

Further search then pointing at square tube with spring force F = 0,2Pcr and F = 0,6Pcr. Fig. 20 shows the energy increment ΔE/κ and the increment ΔW/κ of spring work up to the collapse at two spring force amounts. It seems that the transition of ΔE/κ and ΔW/κ has different pattern of increment energy.

Since the strain energy U at this time becomes larger while F becomes larger, it is considered that the amount of the energy increase becomes different. Comparing the energy absorption, it is obvious that the energy absorption amount (E = W + U_1+ U_2) also increasing. Since the strain energy U (= U_1 + U_2) up to the collapse is not affected by the magnitude of F, the difference in energy absorption is determined by the work W by the spring. Also, exploring for the relationship between the amount of energy absorption and deformation behavior to some extent functions (the elongation of the spring reaches x). Fig. 20 shows the energy absorption becomes possible to absorb more energy when the rectangular tube deforms more base on x amount as shown in Fig. 21.

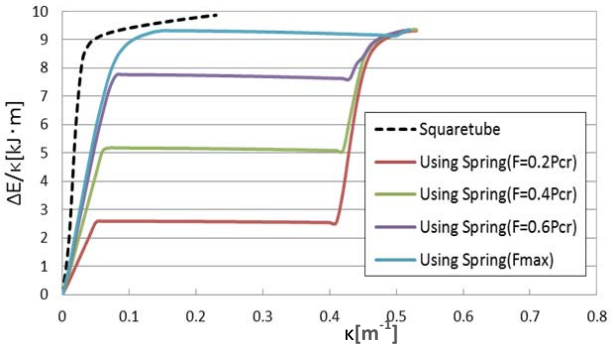

Fig. 22 Increase total energy using F_{max}

IV. Discussion

Fig. 18 shows that increment of the total energy absorption rate ΔE/κ increases while spring force (F) becomes higher. It is a possible to increase total energy since it was affected by spring force (F). Using spring force (F = F_{max}) it produces new deformation and highest total energy even applied at low thickness ratio (t/C_1) as shown in Fig. 22.

Fig. 22 shows that square tube using (F_{max}) produces higher energy compares with determined spring force (F).

V. Conclusion

According to finite element analysis of bending characteristic of square tube conclusion of this study are:

- Square tube with lower spring force produce longer elongation and reduce buckling point at same condition than the others.
- Buckling can be reduced by using lower rigidity force, this correlate with choosing the smaller ratio of load per deflection unit or known as rigidity rate.
- Square tube with higher spring force produces better energy absorption compares with the others at type 1 collapse mode.
- It is possible to increase square tube energy even when using low thickness ratio by install new spring force (F_{max}) which resulted higher energy. In other words, square tube with absorption part proves that it is able to increase

energy absorption at bending test.

ACKNOWLEDGMENT

This project is supported by Strength of Material Laboratory, Yamaguchi University, JSPS KAKENHI Grant Number 26420079, Japan.

REFERENCES

[1] Wang, J. Afshan, S. Schillo, N. Theofanous, M. Feldmann, M. Gardner, L. 2016. Material properties and compressive local buckling response of high strength steel square and rectangular hollow section. International Journal of Engineering Structures, Volume 130, pp297-315.
[2] Chi, K S. Lin, T H. 1977. Slope Deflection Method for Elastic-Plastic Multi-Story Frames. International Journal Solids Structures, Volume 13, pp 125-135.
[3] Stafford, R O. Pattichis, M. 1978. Bending and Torsion of Anisotropic Cantilevers. International Journal of Mechanical Science, Volume 20, pp 395-405.
[4] Wierzbicki, T. Recke, L. Abramowicz, W. Gholami, T. Huang, J. 1994. Stress Profiles In Thin-Walled Prismatic Columns Subjected to Crush Loading – II Bending. Computer and Structures, Volume 51, No 6, pp 625-641.
[5] Kecman, D. 1983. Bending Collapse of Rectangular and Square Section Tubes. International Journal of Mechanical Science, Volume 25, No 9-10, pp 623-636.
[6] Johnson, A F. 1973. Bending and Torsion of Anisotropic Beams. International Journal Solids Structures, Volume 9, pp 527-551.
[7] Kim, T H. Reid, S R. 2001. Bending Collapse of Thin-Walled Rectangular Section Columns. Computer and Structures, Volume 79, pp 1897-1911.
[8] Masuda, K. Chen, D H. Ozaki, S. 2009. Study on Pure Bending Collapse of Square Tubes in Consideration of Work Hardening effect. Transaction of The Japan Society of Mechanical engineers (in Japanese), Volume 75, No 749, pp 13-20.
[9] Masuda, K. Chen, D H. 2009. Study on Role of Partition Plates in Square Tube Subjected to Pure Bending. Transaction of The Japan Society of Mechanical engineers (in Japanese), Volume 75, No 753, pp 38-45.
[10] Haruyama, S. Tanaka, H. Chen, D. H. Khaidir, A. 2012. Study on the Deformation Modes of an Axially Crushed Compact Impact Absorption Member. World Academy of Science, Engineering and Technology, Volume: 6.
[11] Haruyama, S. Khaidir, A. Kaminishi, K. Chen, D H. 2013. Modes of Collapse of Compress-Expand Member Under Axial Loading. World Academy of Science, Engineering and Technology, Volume: 7.